

Bidirectional LED-to-LED communication and energy generator for a VLC-ID access system

R. A. Martínez-Ciro , F. E. López-Giraldo , A. F. Isaza-Piedrahita 

Abstract—This paper presents the development of a bidirectional visible light communication (VLC) system using a 5 mm RGB light-emitting diode (LED), which not only serves as a transmitter and receiver, but also functions as a power generator. A key contribution of this work is the implementation of a power divider using an RGB LED, which simplifies the integration of the optical transceiver and the energy harvesting components. The main objective is to design a visible light communication identification (VLC-ID) system that operates efficiently for access control by leveraging the multifunctionality of RGB LEDs. The system uses on-off keying (OOK) modulation and capacitor based energy storage. An experimental approach is adopted to evaluate the bit error rate (BER) and the accumulated voltage, demonstrating the feasibility of the proposed dual-function VLC-ID system. The key contribution of this work is a power divider circuit that allows each RGB LED to operate in half-duplex mode, simultaneously enabling transmission, reception, and energy harvesting through a single optical channel. This approach simplifies the hardware architecture and supports low-cost, secure access applications.

Index Terms—LED-to-LED communication, Energy harvesting, VLC, LED as sensor, RGB LED, Optical wireless communication.

I. INTRODUCTION

Radio Frequency Identification (RFID) systems are widely used for secure access control, are susceptible to unauthorized interference from external devices that can extract personal information from passive RFID cards [1]. In addition, passive RFID cards can face security risks and performance issues caused by nearby materials, electrical noise, or unauthorized readers. [2]. To overcome these limitations, Visible Light Communication (VLC) has been proposed as a secure and interference-free alternative. By using the visible light spectrum, VLC enables reliable data transmission without affecting existing radio frequency systems, offering a distinct advantage for secure communication [3].

A significant challenge in VLC-based identification systems (VLC-ID) is achieving energy self-sufficiency while maintaining performance levels comparable to passive RFID cards, which are widely used due to their low cost and autonomy. Recent studies on hybrid VLC-RF architectures with lighting-based energy harvesting highlight the importance of optimizing both energy and data efficiency in next generation access control systems [4]. Traditionally, VLC

R. A. Martínez-Ciro, F. E. López-Giraldo and A. F. Isaza-Piedrahita are with the Instituto Tecnológico Metropolitano of Colombia e-mail: rogermartinez@itm.edu.co, franciscolopez@itm.edu.co, andresisaza34307@correo.itm.edu.co.

Manuscript received April 19, 2025; revised August 26, 2025.

systems employ white or RGB LEDs as transmitters and utilize receivers such as photodiodes, solar panels, image sensors, or photoresistors, as summarized in recent reviews of VLC technology [5]. However, these receivers typically allow for only unidirectional communication. Recent research has shown that LEDs can also function as sensors [6, 7] and small solar panels [8]. This multifunctionality allows LEDs to operate in inverse, direct, and photovoltaic regions, which can be harnessed for both communication and energy harvesting. For example, [9] demonstrated that commercial RGB LED bulbs can be used simultaneously for communication, energy harvesting, and environmental sensing, highlighting the growing interest in multifunctional VLC-ID platforms. In this paper, we present a low-cost VLC-ID system for secure access control that uses 5 mm RGB LEDs, an Arduino Nano, and a switching circuit based on Bipolar Junction Transistors (BJTs). The system allows each RGB LED to operate as both a transmitter and a receiver, while simultaneously harvesting and storing energy through a $10\ \mu F$ capacitor [10]. Unlike traditional approaches that require additional power splitters [11–13], our design introduces a novel power divider circuit that integrates bidirectional communication and energy harvesting into a single optical channel. This multifunctionality reduces hardware complexity, improves energy efficiency, and simplifies both hardware and software implementation [14, 15]. The system transmits binary data using on-off keying (OOK) modulation, in which the presence of light represents a binary '1' and its absence a binary '0', a simple and widely used technique in visible light communication systems [16].

The rest of this paper is organized as follows. Section 2 provides a general overview of the LED to LED bidirectional switching system, LED power accumulation and power splitter concept. Section 3 describes the methodology used to measure the BER and energy harvesting. Section 4 shows the mathematical model that predicts the maximum voltage response of each channel of the RGB LED. The overall results are given in Section 5. Finally, the conclusion will be presented in Section 6.

II. PROPOSED SYSTEM OVERVIEW

A. LED switching circuit implementation

The core functionality of the bidirectional VLC-ID system lies in its ability to switch between transmission and reception modes using an RGB LED. Circuit simulations in Proteus 8.13 (Labcenter Electronics Ltd.) confirmed the LED's behavior; however, experimental setups were necessary to validate

its sensing capabilities. The final design incorporated BJT transistors and capacitors for efficient energy storage, enabling the LED to operate as both a transmitter and a receiver. Simultaneously, the other embedded color channels within the same RGB LED were used in photovoltaic mode to harvest energy, allowing the device to perform communication and energy accumulation concurrently without additional optical components.

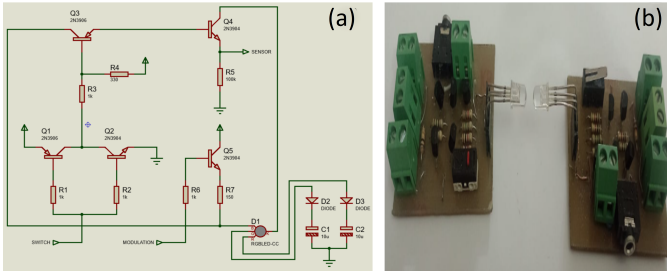


Fig. 1. Bidirectional LED switching circuit for VLC communication and energy harvesting: (a) circuit diagram and (b) experimental prototype.

Inspired by the experiment described in [17], we initially reproduced its setup to explore the unidirectional transmission of audio signals between two LEDs. This exploration guided the design and implementation of a switching circuit for bidirectional communication, resulting in the circuit presented in Fig. 1.

The circuit design includes an RGB LED, a single-pole double throw micro push button, PNP BJT transistors, $10\mu F$ capacitors, and generic diodes. These components are integrated to facilitate the switching between the LED's emitter and receiver functions, while also capturing the energy generated by the other color channels embedded within the same RGB LED.

B. Circuit operation

In the schematic diagram shown in 1a, the switching circuit enables the RGB LED to alternate between transmission and reception modes in a half-duplex configuration. When the push-button is not pressed, a logical '0' is applied to the terminal labeled SWITCH, which reverse-biases the LED, allowing it to operate as a sensor. In this state, the LED is optically sensitive and capable of receiving incoming signals. When the push-button is pressed, a logical '1' is sent to the SWITCH terminal, placing the LED in forward bias and enabling its emission mode. In this configuration, the terminal labeled MODULATION continuously receives the audio signal, but the LED only transmits it when it is forward-biased and illuminated. The BJT transistors in the circuit manage the switching process by selectively enabling current paths depending on the state of the push-button, ensuring correct operation between transmission and reception modes. This ensures that the LED is never electrically connected to both the transmitter and receiver circuits at the same time, thus maintaining proper electrical isolation between transmission and reception. While one module transmits, the

other receives; simultaneous bidirectional communication is not possible, which defines the system as half-duplex.

Simultaneously, the other LEDs embedded within the RGB package continuously accumulate voltage. The diodes in the circuit ensure unidirectional current flow from the LEDs to the storage capacitors, effectively preventing reverse current. This configuration optimizes energy capture, making the stored energy available for later use and enhancing the system's overall energy-harvesting capability.

Fig. 1b illustrates the breadboard implementation of the switching circuit, which was initially designed and simulated using Proteus 8.13 (Labcenter Electronics Ltd.) to validate its functionality before physical fabrication. The simulation ensured correct switching logic and component behavior connections, streamlining the construction process and facilitating experimental testing in the laboratory environment.

C. Communication and energy generation system with Arduino board

A system was developed using an Arduino Nano to control the switching logic between transmission and reception, manage serial data communication through RGB LEDs, and facilitate energy harvesting. As shown in Fig. 2a, the user card is capable of transmitting and receiving data, while also accumulating energy in storage capacitors using the unused LED channels.

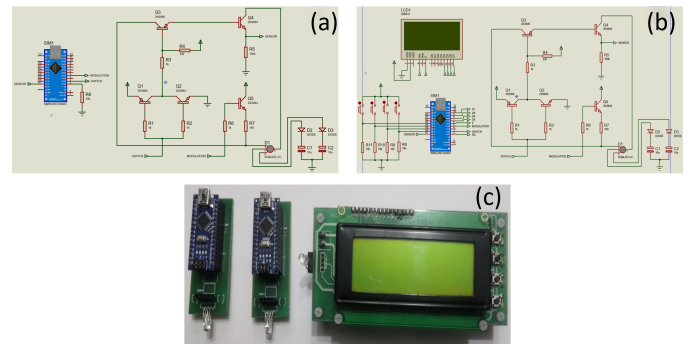


Fig. 2. Design and implementation of the VLC-ID system: (a) key schematic, (b) lock schematic and (c) prototype.

When the push-button on the user card is not pressed, a logical '0' is sent to the SWITCH terminal, keeping the LED in sensor mode. In this state, the signal from transistor Q4 SENSOR is routed to an analog input of the Arduino Nano, allowing it to measure incoming photovoltage. When the button is pressed, a logical '1' is applied to the same terminal, switching the LED to emission mode. In this configuration, the Arduino transmits a serial ASCII data frame, modulated via OOK. The modulating signal is delivered from the Arduino to the MODULATION terminal of the circuit, producing a visible blinking pattern that represents the information. Fig. 2b shows the receiving device, which not only decodes and processes the data sent by the user card but can also send a response, such as a new password, using visible light. This enables bidirectional, half-duplex communication between both modules. While one

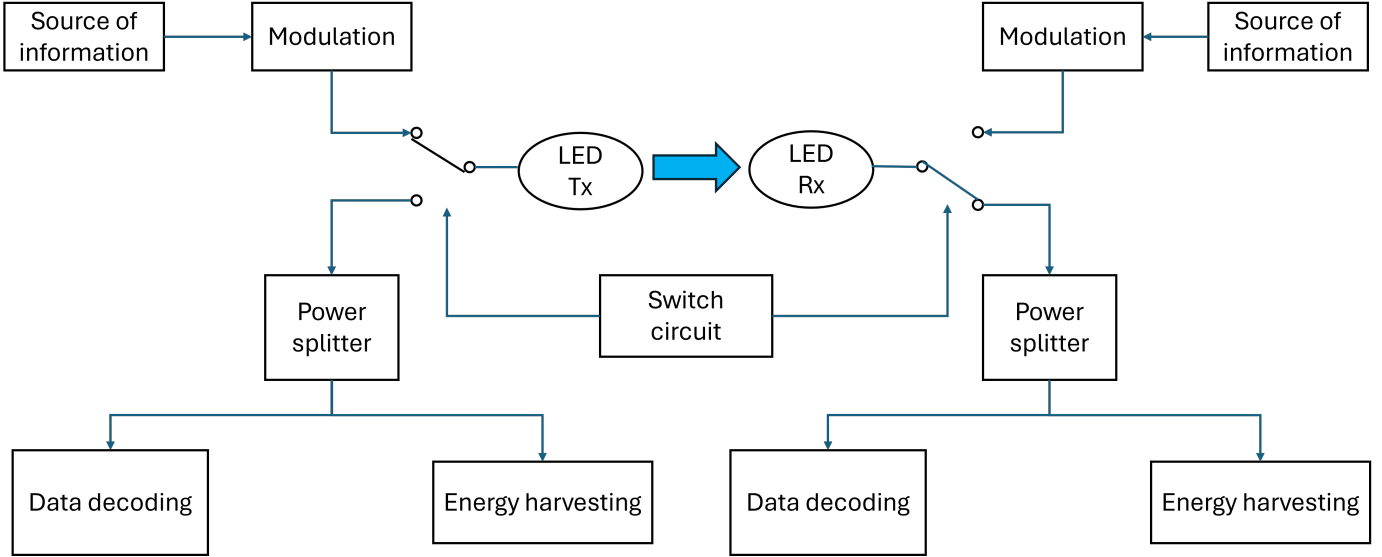


Fig. 3. Conventional power splitting scheme in bidirectional VLC systems.

transmits, the other receives, ensuring proper isolation between modes. Simultaneously, energy harvesting continues through the idle LED channels, enhancing the system's autonomy and efficiency for secure VLC-ID applications.

Fig. 2c illustrates the implementation of the keys and the developed access control system. A printed circuit board (PCB) was constructed for the keys and the receiver to ensure precise and stable connections between the components. The PCB design was carried out using Proteus 8.13 (Labcenter Electronics Ltd.), allowing for simulations and validation of the circuit's functionality prior to physical fabrication.

D. Power splitter system simplification in VLC using RGB LED

As mentioned in the section I, implementing a power splitter within a single LED requires complex hardware and software mechanisms capable of controlling the switching between transmission and reception modes. Moreover, the use of DC-DC converters is necessary to accumulate the voltage generated when the LED operates in its photovoltaic region. In Fig. 3 illustrates a traditional power division scheme used in bidirectional VLC systems. These systems tend to be complex due to the need to alternate between the LED's three functional modes: forward-biased transmission, reverse-biased sensing, and photovoltaic energy harvesting.

To reduce the complexity of traditional power splitters, we propose the use of an RGB LED, where one channel is dedicated to communication (either transmission or reception), and the remaining two channels are used for energy harvesting in photovoltaic mode. This configuration eliminates the need to alternate between data reception and energy accumulation, enabling both functions to operate simultaneously. As shown in Fig. 4, the proposed power splitter model leverages the independent operation of the RGB LED's internal channels. While one channel handles communication, the other two accumulate electrical energy. This separation of functions

within a single RGB LED significantly reduces system complexity and avoids switching delays or interference between modes. By distributing roles across the LED's color channels, the system achieves simultaneous energy harvesting and data communication, enhancing both hardware simplicity and overall efficiency in power-constrained VLC-ID applications.

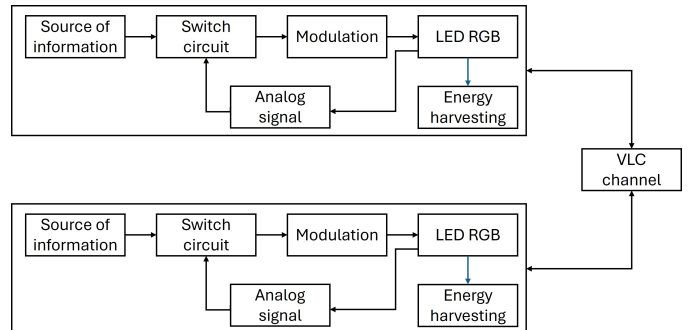


Fig. 4. Simplified power splitting model with RGB LED for simultaneous communication and energy accumulation.

III. MEASUREMENT OF ENERGY HARVESTING AND BER

In this phase, measurements were conducted on the VLC-ID user boards. To evaluate the BER, OOK modulation was applied to a specific channel while the other two channels remained continuously active. The receiver operated on the same channel as the modulating emitter, while the accumulated voltage on the other channels was measured, as shown in Fig. 5.

Voltage values are measured at different distances, ranging from 0 to 140 mm, in 10 mm increments, with the receiver positioned perpendicularly to the emitter. At each distance, five sets of samples are collected for both energy capture and

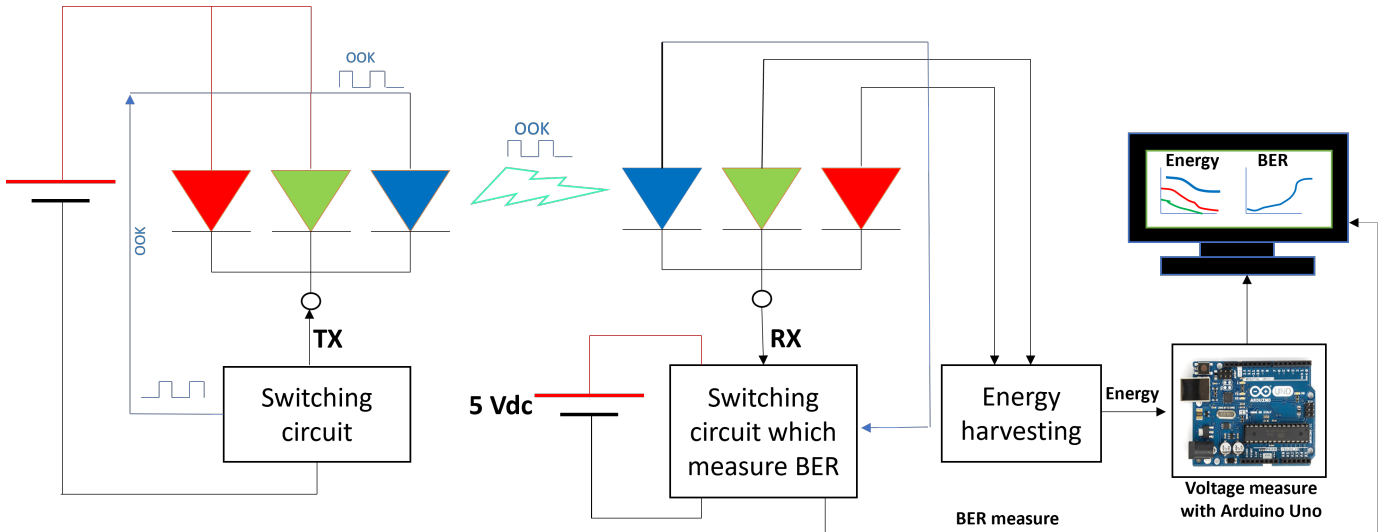


Fig. 5. Experimental setup for BER measurement and voltage accumulation in VLC-ID system.

BER evaluation, and the average of these measurements is calculated for each set.

Data collection is performed using the PLX-DAQ V. 2.11 application, which facilitates serial communication between the embedded Arduino system and Excel. For BER evaluation, measurements are conducted directly on the Arduino Nano used in the switching circuit, operating at a transmission speed of 1200 baud to ensure accurate data transmission. Meanwhile, the accumulated voltage in the capacitors of the remaining channels is measured using an Arduino UNO at 9600 baud. This configuration simplifies the code and avoids unnecessary complexity in programming. In both cases, measurements are taken over a 43-second period, which corresponds to the time required to transmit the preloaded data.

BER measurement and energy collection are performed within the receiver circuit. The software transmits a 2400-bit sequence, with Fig. 6a illustrating the transmission process and Fig. 6b depicting data reception. To ensure accurate energy harvesting measurements, the capacitors are discharged before each new measurement.

IV. MATHEMATICAL MODEL OF THE VLC-ID SYSTEM BASED ON RGB LEDS

A. Mathematical Model for the Receiver

The proposed model aims to predict the voltage response of each channel of the RGB LED used in the VLC-ID system to identify the maximum detection distance of the receiver relative to a given optical power from the transmitter. Based on the state of the art [18, 19], the VLC channel model used is shown in (1):

$$H(d, \theta, \phi) = \begin{cases} \frac{(m+1)A \cos^m(\phi) T_s(\theta) g(\theta) \cos(\theta)}{2\pi d^2} & : \text{if } \theta < \theta_c \\ 0 & : \text{otherwise} \end{cases} \quad (1)$$

In Fig. 7, the schematic of the proposed model shows the system's behavior in relation to the irradiance angle (ϕ) and the incidence angle (θ).

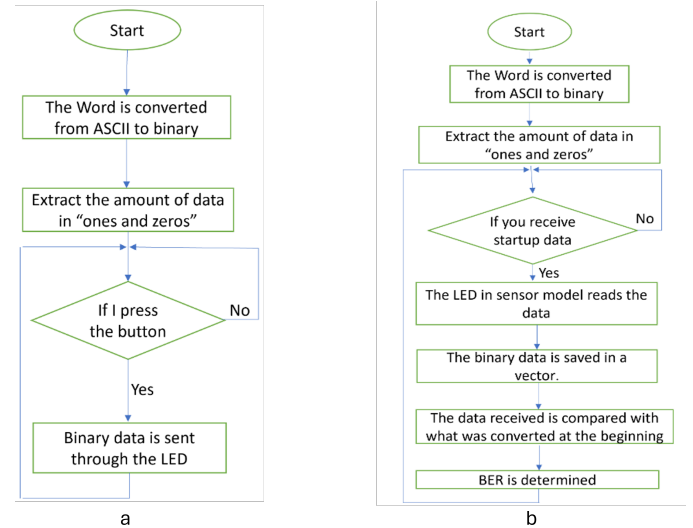


Fig. 6. Data transmission and reception in VLC-ID system: (a) transmission process and (b) received data.

A is the area of the LED detector, d is the distance between the transmitter and receiver, $T_s(\theta)$ is the filter gain, and $g(\theta)$ is a optical concentrator.

The Lambertian coefficient m is calculated using (2), based on the emission half-angle of the LED:

$$m = -\frac{\ln 2}{\ln \cos(\frac{\phi}{2})} \quad (2)$$

Assuming identical emitter and receiver characteristics, the angle can be determined using (3):

$$\cos(\phi) = \frac{h}{d} \quad (3)$$

The distance between the transmitter and the receiver is calculated using (4):

$$d = \sqrt{(M_x - D_x)^2 + (M_y - D_y)^2 + (M_z - D_z)^2} \quad (4)$$

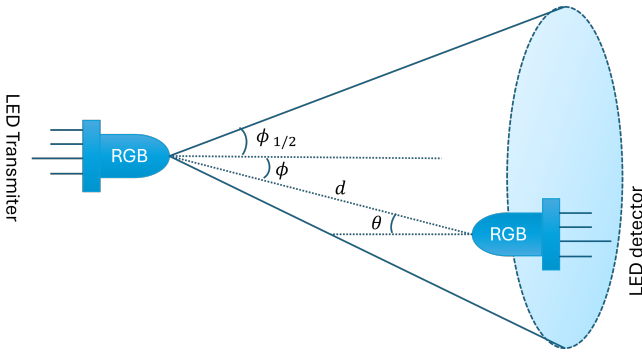


Fig. 7. LED RGB transceiver Model with incidence angle θ and irradiance angle ϕ .

where M_x , M_y and M_z represent the coordinates of the transmitter along the x , y , z axes, respectively, while D_x , D_y and D_z represent those of the receiver.

B. Optical power transmitter and photovoltage of receiver

An implicit variable in the model is the optical power transmitted across the three channels, red transmitted power (P_r), green transmitted power (P_g) and blue transmitted power (P_b). Since measurement equipment was not available to determine its value, the results obtained from the optical power transmitted relative to the current applied to a 5 mm RGB LED, as referenced in [20], were used. The data is tabulated in Excel, and the resulting graph is shown in Fig. 8.

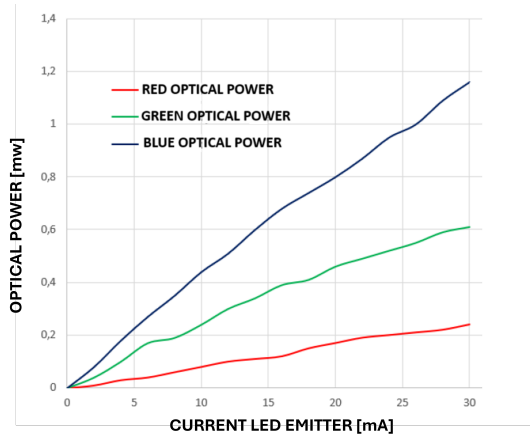


Fig. 8. Current vs. optical power graph for 5mm RGB LED.

From this graph, the equations for the three channels are derived, enabling the determination of power in each channel based on the current consumption of each LED. These expressions are given in (5), (6), and (7):

$$P_r = 0.0083 \times I_{red} \quad (5)$$

$$P_g = 0.0206 \times I_{green} \quad (6)$$

$$P_b = 0.0381 \times I_{blue} \quad (7)$$

The process involves keeping the emitter LED and the receiver aligned at an apparent distance of zero. However, in reality, there is an 8 mm separation due to the capsule

surrounding the LEDs, as shown in Fig. 9. This separation results in the optical concentrator value for the received power not being equal to 1.

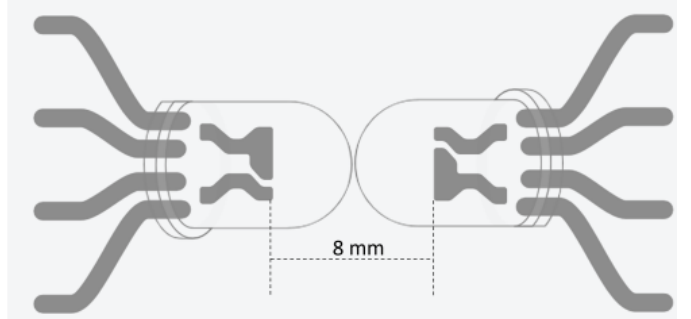


Fig. 9. Distance between LEDs and optical concentration in VLC-ID system.

A power of 1 mW is chosen for the blue LED channel. Therefore, resistors are calculated so that each LED consumes 26 mA. The voltage values for each LED are obtained experimentally, resulting in a voltage of 3.1 V for the blue color, 3.2 V for green, and 2.2 V for red. Using Ohm's law, the resistance values for the red, green, and blue channels are 150 Ω , 90 Ω and 94 Ω , respectively. To obtain the model that relates optical power with generation and communication in the system, voltage measurements are taken at the receiver LED. On the transmitter side, the calculated resistors are connected in series to ensure each LED consumes 26 mA and to generate optical powers of 1 mW for the blue channel, 0.22 mW for the red channel, and 0.54 mW for the green channel. Fig. 10 displays the conceptual diagrams for energy harvesting and communication measurements.

During the transmitter setup, a series of steps is followed. First, the red channel is activated while the others remain off, as shown in Fig. 10a. Voltage is measured across the 1 $M\Omega$ resistors of each channel of the receiver LED using a Fluke 115 digital multimeter in the optics, photonics, and computer vision laboratory at ITM of Medellin. This process is then repeated for the green and blue channels, as illustrated in Figs. 10b and 10c, respectively. The objective is to collect precise experimental data for constructing a mathematical model that describes voltage generation and communication within the system.

The received optical power for each color channel red ($P_{r,r}$), green ($P_{r,g}$) and blue ($P_{r,b}$) is calculated using (8), (9), and (10). The total received optical power (P_t) is then obtained by summing these components, as shown in (11):

$$P_{r,r} = P_r \times H \times T_s \times G_{red} \quad (8)$$

$$P_{r,g} = P_g \times H \times T_s \times G_{green} \quad (9)$$

$$P_{r,b} = P_b \times H \times T_s \times G_{blue} \quad (10)$$

$$P_t = P_{r,r} + P_{r,g} + P_{r,b} \quad (11)$$

The optical filter gain is equal to 1 since the system does not use filters in the receiver, but the optical concentrator gain is different from 1. This is due to the convex curvature of



Fig. 10. Conceptual diagram for voltage measurement in energy harvesting and communication channels.

the RGB LED, which results in a gain in reception that is not the same across all channels because the position of each LED differs. Through adjustments to the model implemented in Matlab software and by comparing it with voltage output measurements from the receiver LED, the following values were found: $G_{red} = 14, 6$; $G_{green} = 5, 34$ and $G_{blue} = 2, 73$.

After acquiring the experimental photovoltage data from each channel, both for energy generation and communication, we proceed to use these data to estimate the output voltage of each channel when receiving a transmitted optical power. While matrix-based approaches have been used in previous studies such as [19], the transformation model used in this work formulated in (12) has been specifically developed and adapted for RGB LED behavior in VLC-ID systems:

$$\begin{bmatrix} V_R \\ V_G \\ V_B \end{bmatrix} = \begin{bmatrix} V_{rr} & V_{gr} & V_{br} \\ V_{rg} & V_{gg} & V_{bg} \\ V_{rb} & V_{gb} & V_{bb} \end{bmatrix} \cdot \begin{bmatrix} P_{r,r} \\ P_{r,g} \\ P_{r,b} \end{bmatrix} \quad (12)$$

let V_R , V_G and V_B be the voltage signals corresponding to

each channel of the RGB LED, where:

- V_R represents the voltage in the red channel,
- V_G represents the voltage in the green channel,
- V_B represents the voltage in the blue channel,

Additionally, we define V_{ij} , where i and j correspond to the channels of the transmitting LED, such that i represents the transmitting channel and j the receiving channel. This notation allows us to analyze the interaction of voltages between the different channels of the RGB LED, which is essential for the operation of the proposed system.

By substituting the measured gains into (12), we obtain the output voltages as expressed in (13):

$$\begin{aligned} V_R &= (0.1932 \times P_{r,r}) + (1.3270 \times P_{r,g}) + (0.3420 \times P_{r,b}) \\ V_G &= (0.0009 \times P_{r,r}) + (0.2300 \times P_{r,g}) + (4.5200 \times P_{r,b}) \\ V_B &= (0.0001 \times P_{r,r}) + (0.0001 \times P_{r,g}) + (0.0450 \times P_{r,b}) \end{aligned} \quad (13)$$

C. Mathematical model of the receiver in OOK communication

In VLC systems based on OOK modulation, the receiver plays a critical role in interpreting the modulated signals transmitted by the emitter. The mathematical model of the receiver is essential to understand how the received signal is processed, how information is detected, and how the quality of the communication is assessed. This model serves as the basis for assessing the system's performance in terms of detection accuracy and its ability to withstand noise and channel distortions.

This section focuses on the development of the model in Matlab software that describes the behavior of the receiver LED using OOK modulation. The input variables include the transmission of binary data, the distance between the emitter and the receiver, as well as the beta value of the employed transistor. During the transmission stage, 2400 random bits were sent at a rate of 1200 baud, using the RS-232 communication protocol.

Based on the experimental results presented in Section III, it was observed that the blue channel demonstrated the most stable behavior in communication mode, while the red LED produced the highest voltage when all channels were active. This insight served as the starting point for the model's development. In the transmitter, the red and green channels are continuously activated to generate 0.22 mW and 0.54 mW, respectively, while OOK modulation is applied to the blue channel, leading to the transmitter equation outlined in (14):

$$\begin{aligned} P_r &= 0.0083 \times (I_r) \\ P_g &= 0.0206 \times (I_g) \\ P_b &= 0.0381 \times (I_b) \times \text{OOK} \end{aligned} \quad (14)$$

The electrical noise in the receiver circuit is calculated by considering the transducer noise (η_{rms}) and the offset noise at the transistor output V_{DC} , as shown in (15):

$$n_t = (\eta_{rms} P_r + V_{DC}) \quad (15)$$

Based on the noise and offset voltage measurements at the transistor output 329.5 mV, and 3.6 mV, respectively, the modulation voltage in each channel is calculated as shown in (16):

$$\begin{aligned} V_R &= V_r + n_t \\ V_G &= V_g + n_t \\ V_B &= V_b + n_t \end{aligned} \quad (16)$$

Finally, the output voltage in the blue channel, which is used for communication, is analyzed. This channel differs from the other channels because the communication channel output is an **Analog output** through a BJT transistor, as shown in the Fig. 11. The corresponding calculations are also performed for the transistor.

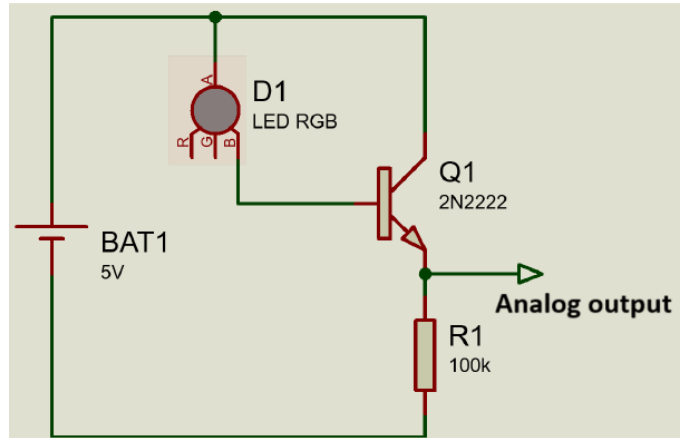


Fig. 11. LED sensor conditioning for VLC-ID communication.

V. RESULTS OF ENERGY HARVESTING AND COMMUNICATION

A. Red channel: Energy harvesting and communication

In Fig. 12, the results of the energy harvesting for the green and blue channels are presented, as well as the communication for the red channel.

Fig. 12(a) shows the voltage accumulation in two 10 μF capacitors connected to the green and blue channels. The data obtained indicate the following observations:

- Green channel: The evaluation reveals that the green channel does not reach a voltage higher than 1 V, suggesting that this wavelength is not suitable for energy harvesting applications in the VLC-ID system. This result indicates that the green channel does not efficiently accumulate energy and is therefore not a viable option for optimizing the VLC-ID system in terms of energy generation and storage.
- Blue channel: Voltage accumulation in the blue channel was also evaluated within the VLC-ID system. The generated voltage was lower than that of the green channel, suggesting that, despite its potential applications in other contexts, it is not suitable for optimizing energy accumulation in this system.

Fig. 12(b) illustrates the relationship between BER (Bit Error Rate) and distance in the red channel during data transmission:

- Response at Short Distances: At short distances, when the transmitter sends data through the red channel while the other channels are active, sensor saturation is observed. This saturation prevents the correct reception and decoding of data.
- Response at Greater Distances: At an approximate distance of 20 mm, the red LED starts functioning as a sensor and provides a detectable response. However, data decoding at this distance is still not accurate. This suggests that although the red channel is capable of receiving data, the quality of communication and decoding accuracy need improvement, especially at greater distances.

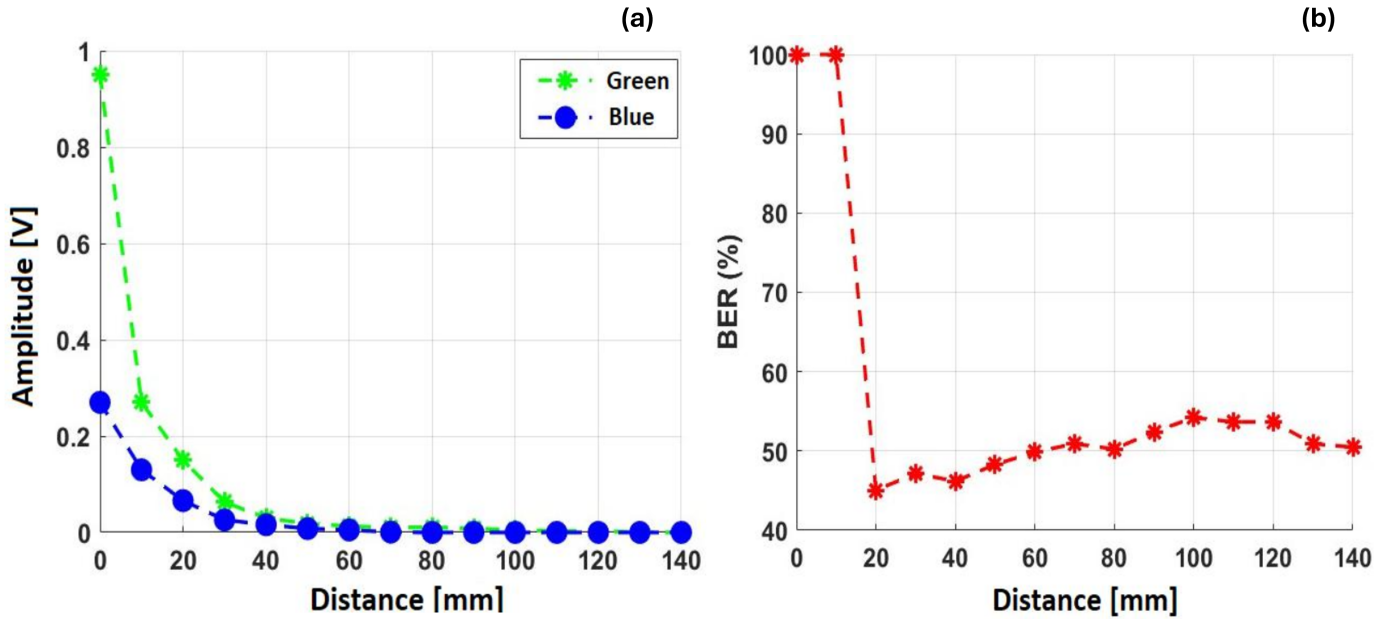


Fig. 12. The results obtained for the voltage generated by the LED and the BER: (a) Energy harvesting in the green and blue channels and (b) Communication in the red channel.

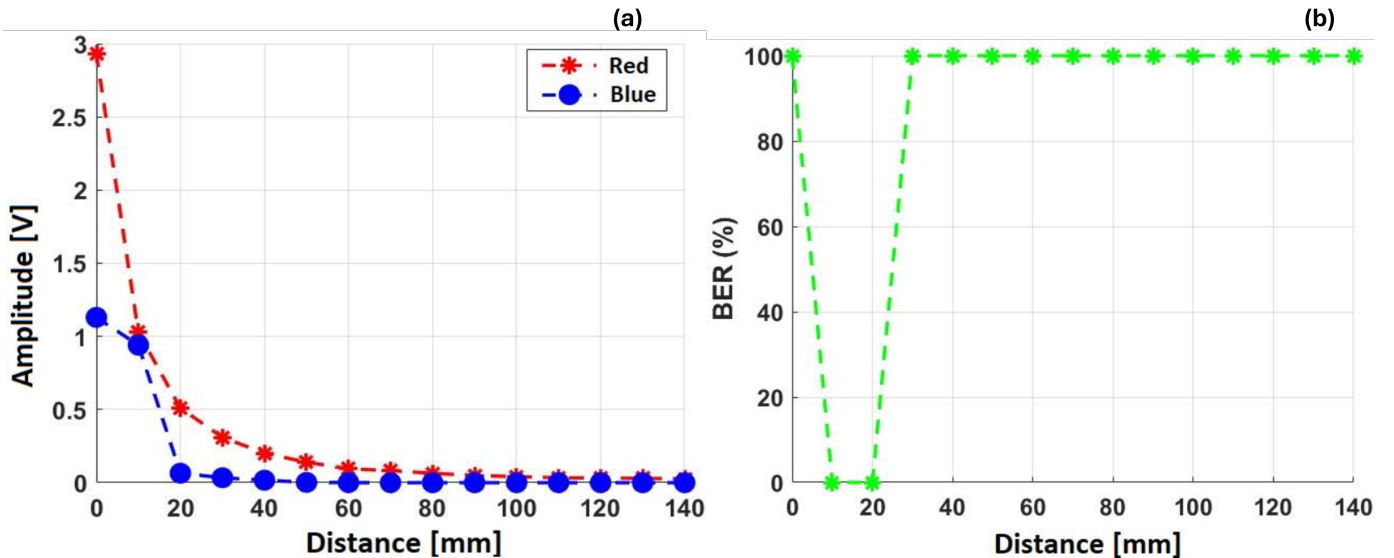


Fig. 13. The results obtained for the voltage generated by the LED and the BER: (a) Energy Harvesting in the red and blue channels and (b) Communication in the green channel.

B. Green channel: Energy Harvesting and Communication

In Fig. 13, the response of the red and blue channels in energy harvesting mode and the green channel in communication mode is observed.

Fig. 13a shows the voltage accumulation in two $10 \mu\text{F}$ capacitors connected to the red and blue channels. The obtained data indicate the following observations:

- Red channel: This channel demonstrates the ability to generate an average voltage of 3 V at short distances. This performance is suitable for low-cost applications, aligning with the goal of developing a system model that integrates energy harvesting. The red channel's ability

to provide usable voltage at short distances could be useful for VLC-ID applications requiring economical and compact solutions.

- Blue channel: Contrary to what is investigated in the state of the art, the blue channel does not show usable voltage generation in this context. This highlights the importance of adjusting the design and components of the VLC-ID system to maximize energy efficiency, as the blue channel does not meet the energy harvesting expectations in this specific case.

Fig. 13(b) shows the BER related to the green channel, evaluated at different distances:

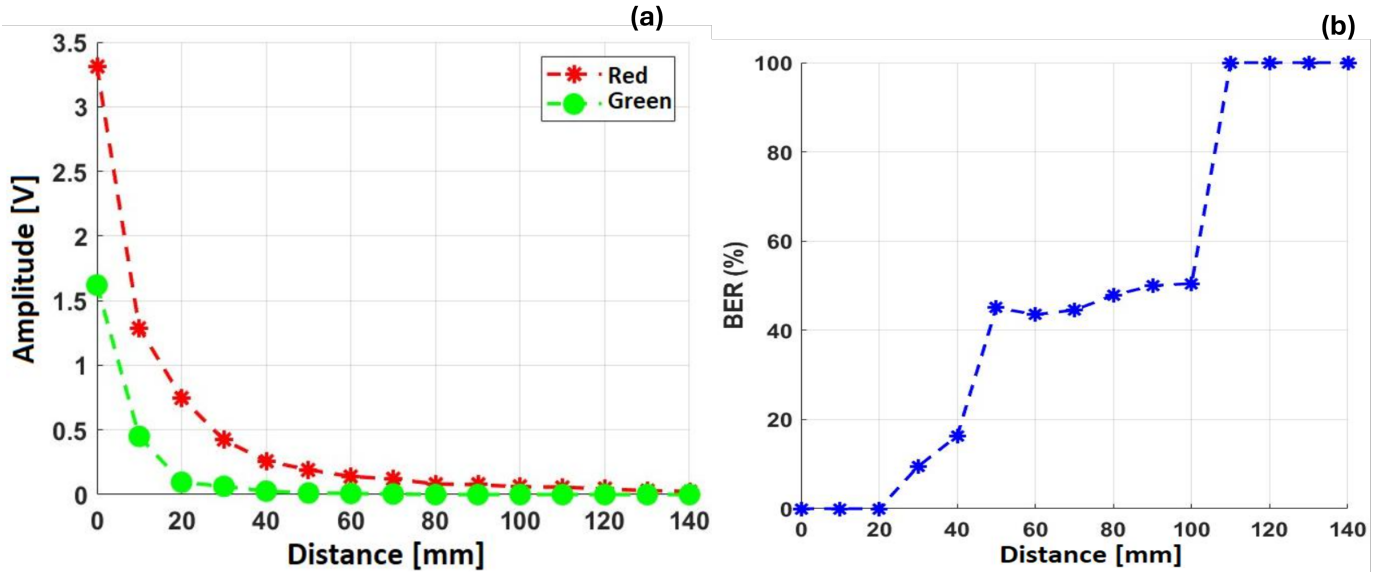


Fig. 14. The results obtained for the voltage generated by the LED and the BER: (a) Energy Harvesting in the green and red channels and (b) Communication in the blue channel.

- Short Distances: At short distances, the green channel does not achieve effective data reception, indicating potential communication issues at close ranges.
- Optimal Range ($10 - 20\text{ mm}$): Between 10 and 20 mm , the green channel achieves optimal performance with a BER of 0% . This finding is crucial for validating the proposed model for data transmission in VLC-ID systems, as it suggests that the green channel can offer precise and reliable communication within this range.
- Greater Distances ($> 20\text{ mm}$): At distances greater than 20 mm , data reception is compromised again. This result indicates the need to optimize the VLC-ID system to maintain effective communication at greater distances, possibly by adjusting the system design or communication parameters.

C. Blue channel: Energy Harvesting and Communication

Fig. 14 illustrates the response of the red and green channels in harvesting mode and the blue channel in communication mode.

Fig. 14a shows the voltage accumulation in two $10\text{ }\mu\text{F}$ capacitors connected to the red and green channels. The obtained data indicate the following observations.

- Red channel: In this configuration, the red channel achieves an average voltage of 3.35 V . This result is significant for developing the energy harvesting model in the VLC-ID context, as it indicates that the blue channel is not as efficient in energy generation compared to the red and green channels. The capability of the red and green channels to generate higher voltages is crucial for optimizing the VLC-ID system, which may lead to design adjustments to maximize harvesting efficiency.
- Green channel: The green channel accumulates 1.5 V , which is a positive result for energy harvesting. This voltage is adequate and necessary for the effective

implementation of these techniques in the VLC-ID system.

Regarding communication, Fig. 14(b) shows that the blue channel, when functioning as a sensor, demonstrates optimal performance for VLC-ID communication applications:

- BER of 0% : The blue channel exhibits a BER of 0% up to distances of 20 mm , ensuring accurate data transmission and detection within this range. This performance is relevant for validating the proposed model for LED communication in VLC-ID systems, confirming that the blue channel is effective in maintaining reliable communication at short distances.
- Limitations at Greater Distances: Although the blue channel is effective at short distances, its communication capability at greater distances may require additional adjustments to the system. These results suggest that for VLC-ID applications involving greater distances, it may be necessary to optimize the system to enhance communication or consider alternative design approaches.

VI. CONCLUSIONS

This research demonstrates the feasibility of a bidirectional VLC-ID system using 5 mm RGB LEDs for simultaneous communication and energy harvesting. The system achieved efficient data transmission at 250 kbps , while generating up to 3 V on the red channel and 1 V on the green channel, confirming its capability for effective energy generation and storage. The blue channel proved to be the most suitable for data transmission, achieving a 0% bit error rate (BER) at distances up to 20 mm , while the red channel proved optimal for energy harvesting. However, communication performance deteriorated at greater distances, highlighting the need for design improvements to extend the effective transmission range.

The proposed system provides a practical, low-cost, and energy-efficient solution for secure access control applications by integrating bidirectional communication and energy harvesting into a single RGB LED.

Further research should focus on enhancing the transmission range through optimized circuit designs and advanced modulation schemes. Additionally, exploring higher-efficiency materials for photovoltaic energy conversion and integrating adaptive control algorithms could further improve system performance. Other enhancements could include increasing the emitted optical power through the use of optical lenses, more efficient RGB LEDs, or optimized driving current profiles. Integrating this VLC-ID system with IoT devices in smart access networks presents a promising avenue for continued development and real world deployment.

REFERENCES

- [1] A. K. Singh and B. Patro, "Security attacks on rfid and their countermeasures," in *Computer Communication, Networking and IoT: Proceedings of ICICC 2020*. Springer, 2021, pp. 509–518, https://doi.org/10.1007/978-981-16-0980-0_49.
- [2] C. Munoz-Ausecha, J. Ruiz-Rosero, and G. Ramirez-Gonzalez, "Rfid applications and security review," *Computation*, vol. 9, no. 6, p. 69, 2021, <https://doi.org/10.3390/computation9060069>.
- [3] L. E. M. Matheus, A. B. Vieira, L. F. Vieira, M. A. Vieira, and O. Gnawali, "Visible light communication: concepts, applications and challenges," *IEEE Communications Surveys & Tutorials*, vol. 21, no. 4, pp. 3204–3237, 2019, <https://doi.org/10.1109/COMST.2019.2913348>.
- [4] Y. Guo, K. Xiong, Y. Lu, D. Wang, P. Fan, and K. B. Letaief, "Achievable information rate in hybrid vlc-rf networks with lighting energy harvesting," *IEEE Transactions on Communications*, vol. 69, no. 10, pp. 6852–6864, 2021, <https://doi.org/10.1109/TCOMM.2021.3098030>.
- [5] S. N. Ismail and M. H. Salih, "A review of visible light communication (vlc) technology," in *AIP Conference Proceedings*, vol. 2213, no. 1. AIP Publishing, 2020, <https://doi.org/10.1063/5.0000109>.
- [6] L. Incipini, A. Belli, L. Palma, M. Ballicchia, and P. Pierleoni, "Sensing light with leds: performance evaluation for iot applications," *Journal of Imaging*, vol. 3, no. 4, p. 50, 2017, <https://doi.org/10.3390/jimaging3040050>.
- [7] F. Leccese and G. S. Spagnolo, "Led-to-led wireless communication between divers," *Acta IMEKO*, vol. 10, no. 4, pp. 80–89, 2021, https://doi.org/10.21014/acta_imeko.v10i4.1177.
- [8] G. M. Pour and W. D. Leon-Salas, "Solar energy harvesting with light emitting diodes," in *2014 IEEE International Symposium on Circuits and Systems (ISCAS)*. IEEE, 2014, pp. 1981–1984, <https://doi.org/10.1109/ISCAS.2014.6865551>.
- [9] M. S. Mir, B. Majlesein, B. G. Guzman, J. Rufo, and D. Giustiniano, "Rgb led bulbs for communication, harvesting and sensing," in *2022 IEEE International Conference on Pervasive Computing and Communications (PerCom)*. IEEE, 2022, pp. 180–186, <https://doi.org/10.1109/PerCom53586.2022.9762392>.
- [10] V. Lange and R. Hönl, "Led as transmitter and receiver in pof-based bidirectional communication systems," in *2018 International IEEE Conference and Workshop in Óbuda on Electrical and Power Engineering (CANDO-EPE)*. IEEE, 2018, pp. 000 137–000 142, <https://doi.org/10.1109/CANDO-EPE.2018.8601162>.
- [11] A. R. Ndjiongue and T. M. Ngatche, "Led-based energy harvesting systems for modern mobile terminals," in *2020 International Symposium on Networks, Computers and Communications (ISNCC)*. IEEE, 2020, pp. 1–6, <https://doi.org/10.1109/ISNCC49221.2020.9297232>.
- [12] P. D. Diamantoulakis and G. K. Karagiannidis, "Simultaneous lightwave information and power transfer (slipt) for indoor iot applications," in *GLOBECOM 2017-2017 IEEE Global Communications Conference*. IEEE, 2017, pp. 1–6, <https://doi.org/10.1109/GLOCOM.2017.8254781>.
- [13] I. Haydaroglu and S. Mutlu, "Optical power delivery and data transmission in a wireless and batteryless microsystem using a single light emitting diode," *Journal of Microelectromechanical Systems*, vol. 24, no. 1, pp. 155–165, 2014, <https://doi.org/10.1109/JMEMS.2014.2323202>.
- [14] X. Fan, W. D. Leon-Salas, T. Fischer, and A. Perez-Olvera, "An led-based image sensor with energy harvesting and projection capabilities," in *2016 IEEE SENSORS*. IEEE, 2016, pp. 1–3, <https://doi.org/10.1109/ICSENS.2016.7808901>.
- [15] W. D. Leon-Salas and X. Fan, "Photo-luminescence modulation circuits for solar cell based optical communications," in *2019 IEEE International Symposium on Circuits and Systems (ISCAS)*. IEEE, 2019, pp. 1–5, <https://doi.org/10.1109/ISCAS.2019.8702596>.
- [16] P. A. Loureiro, F. P. Guiomar, and P. P. Monteiro, "Visible light communications: A survey on recent high-capacity demonstrations and digital modulation techniques," in *Photonics*, vol. 10, no. 9. MDPI, 2023, p. 993, <https://doi.org/10.3390/photonics10090993>.
- [17] M. Hasegawa, "Satisfactory role of leds as a light receiving component and their uses in science demonstration experiments for educational purposes," in *Education and Training in Optics and Photonics*. Optica Publishing Group, 2019, p. 11143_79, <https://doi.org/10.1117/12.2523733>.
- [18] F. A. Dahri, F. A. Umraní, A. Baqai, and H. B. Mangrio, "Design and implementation of led-led indoor visible light communication system," *Physical communication*, vol. 38, p. 100981, 2020, <https://doi.org/10.1016/j.phycom.2019.100981>.
- [19] R. A. Martínez-Ciro, F. E. López-Giraldo, A. F. Betancur-Perez, and J. M. Luna-Rivera, "Design and implementation of a multi-colour visible light communication system based on a light-to-frequency

- receiver,” in *Photonics*, vol. 6, no. 2. MDPI, 2019, p. 42, <https://doi.org/10.3390/photonics6020042>.
- [20] M. Galal, W. P. Ng, R. Binns, and A. Abd El Aziz, “Characterization of rgb leds as emitter and photodetector for led-to-led communication,” in *2020 12th International Symposium on Communication Systems, Networks and Digital Signal Processing (CSNDSP)*. IEEE, 2020, pp. 1–6, <https://doi.org/10.1109/CSNDSP49049.2020.9249617>.



Francisco Eugenio López Giraldo received the B.Sc. degree in Physics on Quantum Optics in 2003, the M.Sc. degree in Physics on Many-Body Interactions in Semiconductors in 2007 and Ph.D in Physics on Semiconductor Nanostructures in 2009 from the Antioquia University of Colombia. During his Ph.D. studies in Semiconductor Nanostructures at the Antioquia University (2006 - 2009), he study of electronic and optic properties of semiconductor nanostructures, specifically the Landè g Factor. In 2008, he worked in UNICAMP on Optical Properties of Semiconductor Heterostructures. He is currently a research professor at engineering faculty of the Metropolitan Institute of Technology, Colombia since 2009. His research interests includes Antennas, Wireless Communication and Visible Light Communication.



Roger Alexander Martínez Ciro received the bachelor’s degree in telecommunication engineering, the master’s degree in automation and industrial control and the Ph.D. degree in Engineering from the Metropolitan Institute of Technology of Medellín, Colombia in 2015, 2018 and 2023 respectively. He is currently a research professor at engineering faculty of the Metropolitan Institute of Technology, Colombia since 2018. His research interests includes Optical Wireless Communication, Indoor Positioning and Visible Light Communication.



Andres Felipe Isaza received the bachelor’s degree in Electromechanical Engineering and the master’s degree in Automation and industrial control from the Metropolitan Institute of Technology of Medellín, Colombia in 2013 and 2025 respectively. He is currently research group coordinator and professor at the Faculty of Engineering of the Institute University Pascual Bravo since 2013 and 2020 respectively. His research interests include Energy Harvesting, Visible Light Communication, and Industrial Automation and Control.